Proceedings of the 4th International Conference on Mechatronics and Smart Systems
DOI: 10.54254/2755-2721/2026.33434

Analysis of the Evolution of Urban Heat Island Effect and Its Land Driving Forces in Yinchuan City Based on Landsat Imagery

Kunheng Wu

College of Design and Engineering, National University of Singapore, Singapore, Singapore
E1310990@u.nus.edu

Abstract. Based on four phases of Landsat remote sensing imagery from 2010, 2015, 2020 and 2025, this paper analyses the spatiotemporal evolution of the urban heat island (UHI) effect and the driving mechanism of land cover in Yinchuan City over the recent 15 years. The study retrieves land surface temperature (LST) from USGS L2SP products and classifies heat island intensity (HII) using the mean-standard deviation method. The results show that the UHI in Yinchuan City presents a dumbbell-shaped spatial pattern, with high temperatures concentrated in the northwest and southeast ends and a low-temperature zone in the central area. From 2010 to 2025, the overall HII trend shows fluctuation, intensification, and decline, mainly driven by the combined effects of seasonal climate and urban expansion. Specifically, the expansion of construction land and industrial agglomeration significantly intensifies the local thermal environment, while wetlands and ecological restoration projects alleviate extremely high-temperature events to some extent. These findings provide an important reference for regulating the urban thermal environment and eco-city planning in arid oasis cities.

Keywords: Urban Heat Island Effect, Landsat Remote Sensing, Land Surface Temperature, Land Cover Change

1. Introduction

Since the start of the 21st century, rapid global urbanisation has profoundly altered the physical properties of natural land surfaces. As large areas of natural vegetation, wetlands and farmland are replaced by impervious surfaces, the heat capacity, thermal conductivity and albedo of urban areas have undergone fundamental changes. This leads to significantly higher temperatures in urban areas than in surrounding suburban regions, forming the typical urban heat island effect [1]. This thermal environmental problem not only increases urban energy consumption for cooling in summer but also exacerbates air pollution and health risks for residents and has become a key ecological issue restricting the sustainable development of cities [2]. Yinchuan, a typical arid and semi-arid oasis city, has experienced built-up area expansion and industrial agglomeration in recent years, which have altered the surface energy and water processes. Coupled with the composite geomorphology formed by the Helan Mountains, the Yellow River, and lake wetlands, the city's urban thermal

© 2026 The Authors. This is an open access article distributed under the terms of the Creative Commons Attribution License 4.0 (https://creativecommons.org/licenses/by/4.0/).

DOI: 10.54254/2755-2721/2026.33434

environment exhibits strong spatial heterogeneity [3]. Traditional research methods that rely on meteorological stations or field measurements at a small number of sample points often face limitations, including sparse observation points, insufficient spatial coverage, and difficulty in depicting differences between heat sources and wetland cold islands. These limitations can easily lead to misjudgments about the intensity and scope of the heat island, which in turn cause errors in the layout of ventilation corridors and blue-green spaces, deviations in land-use management and control, and increases in summer cooling energy consumption and health risks from heat exposure.

To address these shortcomings, this paper uses multi-temporal Landsat imagery and obtains consistent LST data from the L2SP LST products released by USGS. Meanwhile, to account for background temperature differences caused by variations in imaging seasons, the mean-standard deviation method is used to standardise and classify HII, thereby enabling relative comparability of multi-temporal UHI results. This technical route, relying on long-term remote sensing data with a 30 m spatial resolution, can construct a continuous surface thermal field at the urban scale. Compared with traditional point-based observation, it is more conducive to identifying the aggregation, expansion and fusion processes of thermal patches. At the same time, the standardised classification method can effectively reduce the noise interference caused by seasonal differences, making the comparison of UHI changes across different time scales more interpretable. It can also be coupled with land cover and land use analysis to quantitatively assess the drivers of construction land expansion, industrial heat source intensification, and wetland cooling regulation on the thermal environment, thereby providing more targeted and practical significance for heat risk management and ecological planning.

Remote sensing-based UHI research has gradually evolved from early single-phase temperature mapping to multi-phase comparative analysis, and further to long-term evolution monitoring and analysis of driving mechanisms. The research focus has also shifted from identifying the existence of UHI to explaining how UHI is reshaped by urbanisation processes and informing management decisions, with the methodological system expanding from simple threshold-based division to product-based LST retrieval, standardised comparison, and coupling analysis with land cover. On this basis, this paper takes Yinchuan City as the research object. It sequentially carries out LST acquisition and UHI classification, characterisation of UHI spatial patterns and temporal evolution, and analysis of the driving forces of land cover change. It aims to answer the core question of how urban expansion and industrial and ecological patterns jointly shape the thermal environment of Yinchuan, and to provide an operational quantitative basis and empirical reference for ecological restoration, blue-green space optimisation, and planning decisions of arid oasis cities.

2. Materials and methods

2.1. Overview of the study area

Yinchuan City is located in the central part of the Ningxia Plain in northwest China, bordering the Helan Mountains to the west and the Yellow River to the east. It is the capital city of the Ningxia Hui Autonomous Region. The study area has a terrain that is high in the west and low in the east, showing a stepped distribution. The western part consists of the Helan Mountains and alluvial fans, the central part is the vast Yinchuan Plain, and the eastern part is the Yellow River alluvial plain. This unique geographical pattern, with mountains backing the city and water facing it, creates a natural thermal environment background for Yinchuan. The exposed Gobi Desert beaches in the western part often serve as natural high-temperature heat sources in summer. At the same time, the eastern plain is relatively cool due to its well-developed water system [3].

DOI: 10.54254/2755-2721/2026.33434

As the core city of the Yellow River Urban Belt, Yinchuan City presents a distinct three-district spatial structure. Xingqing District, the old urban commercial centre, has a dense population and extremely high building density. Jinfeng District, the administrative centre and modern new urban area, has seen the most rapid urban construction and expansion in recent years. Xixia District houses the city's major higher education parks and industrial zones [4,5]. Notably, Yinchuan has long been known as the Lake City in the Frontier, with a wetland ecosystem of the Seventy-two Connected Lakes formed by Yuehai Lake, Qizi Lianhu Lake, Diannong River and other water bodies within the city. These water systems and wetlands running through the city have not only reshaped the urban landscape, but also act as important cold island corridors, playing a key role in regulating the urban microclimate and mitigating the UHI effect [6].

2.2. Data sources and preprocessing

2.2.1. Selection of remote sensing data

To reveal the evolution law of the UHI effect in Yinchuan City over the recent 15 years, this study selects Landsat series satellite imagery released by the United States Geological Survey (USGS) as the main data source. Considering the periodicity of urban construction and data availability, four phases of imagery from 2010, 2015, 2020 and 2025 are selected respectively (Figures 1 and 2).

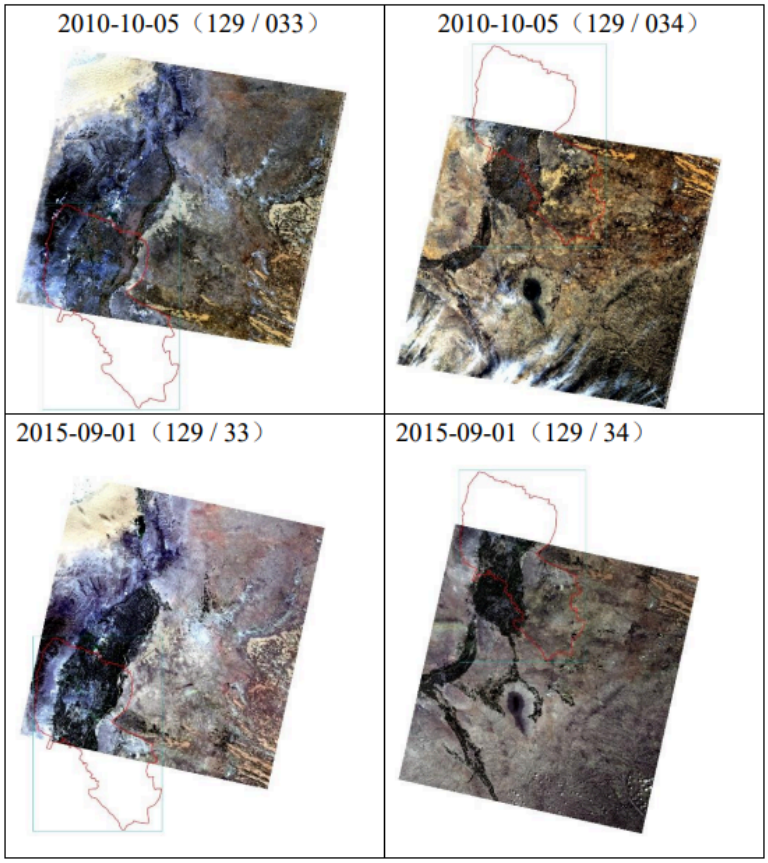

Figure 1. Original remote sensing images

DOI: 10.54254/2755-2721/2026.33434

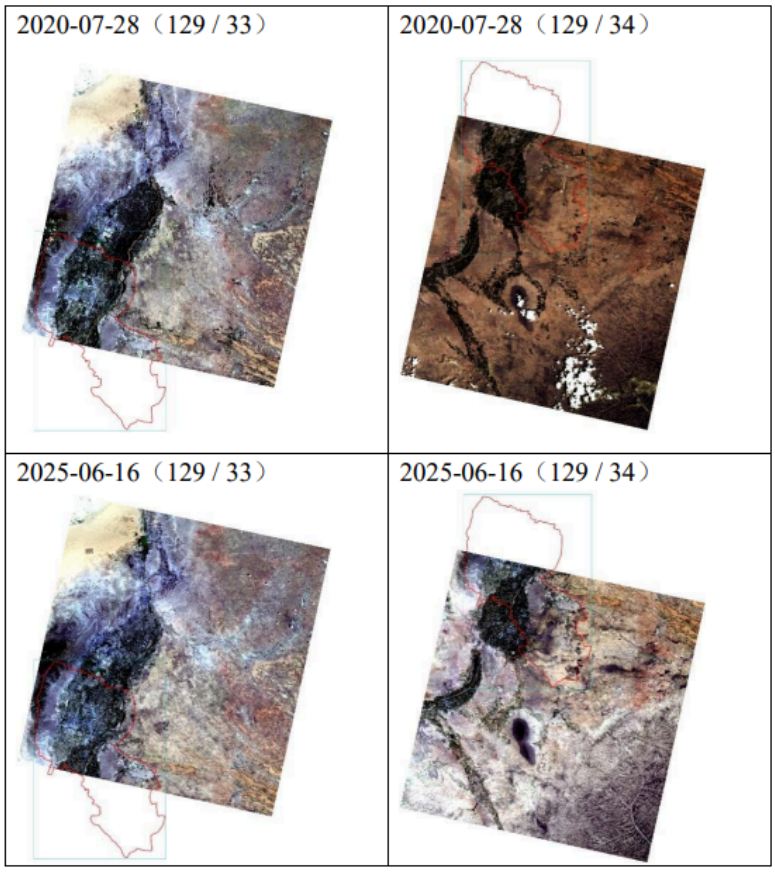

Figure 2. Original remote sensing images

2.2.2. Data preprocessing

This study directly adopts the Collection 2 Level-2 Science Product (L2SP) released by USGS. Before distribution, this product has undergone official radiometric calibration and atmospheric correction. It directly includes bands for surface reflectance and land surface temperature (LST), which greatly improves the quantitative accuracy and processing efficiency of the data.

On the ENVI platform, the main preprocessing steps are as follows. Image mosaicking: Yinchuan City covers two Landsat path/row strips (129/033 and 129/034), so histogram matching technology is applied to realise seamless mosaicking of the northern and southern image scenes. Study area cropping: A vector map of Yinchuan City's administrative boundary is used to mask the mosaicked imagery.

2.3. LST retrieval and classification methods

2.3.1. LST retrieval

Unlike traditional retrieval methods based on the Radiative Transfer Equation (RTE), this study directly obtains LST from the ST band of the L2SP product. Generated with a single-channel algorithm, this product delivers high retrieval accuracy. The raw data are scaled values of Kelvin temperature, which need to be converted to Celsius degrees using the following formula:

$$T_s = (DN \times 0.00341802 + 149.0) - 273.15 \quad (1)$$

DOI: 10.54254/2755-2721/2026.33434

Where T_s is the land surface temperature (℃), DN is the image pixel value, 0.00341802 is the scaling factor, and 149.0 is the offset.

2.3.2. Classification of heat island intensity levels

The four selected image scenes were acquired in June, July, September and October, respectively, leading to substantial differences in solar radiation intensity and atmospheric background temperature across seasons. Direct comparison of absolute temperature values thus cannot objectively reflect the evolution trend of heat island intensity. For this reason, this study adopts the mean-standard deviation method to standardise and classify heat island intensity. This method takes the mean temperature (μ) and standard deviation (σ) of each image scene as the benchmark, and divides LST into 5 levels (Table 1). It eliminates the influence of seasonal background temperature, enabling comparability of heat island spatial patterns across different phases [7].

Table 1. Classification criteria for heat island intensity levels

Level	Name	Classification Threshold (Ts)
1	Strong Green Island Zone	$T_s \leq \mu - 1.0\sigma$
2	Green Island Zone	$\mu - 1.0\sigma < T_s \leq \mu - 0.5\sigma$
3	Normal Zone	$\mu - 0.5\sigma < T_s \leq \mu + 0.5\sigma$
4	Heat Island Zone	$\mu + 0.5\sigma < T_s \leq \mu + 1.0\sigma$
5	Strong Heat Island Zone	$T_s > \mu + 1.0\sigma$

2.4. Land use classification

To explore the driving mechanism of urban expansion on the thermal environment, this study extracts land-use information from Landsat imagery using a Support Vector Machine (SVM)- based supervised classification method. Based on the study area's actual conditions, a classification system is established that covers cropland, construction land, water bodies, forest land, grassland, and bare land.

2.5. Technical route for spatiotemporal analysis of heat islands

After completing LST retrieval and heat island intensity classification, the LST raster data for each year are first imported into a GIS platform for spatial statistics and visualisation of temperature data within the study area. Based on the five heat island levels classified by the mean-standard deviation method, a corresponding urban heat island intensity distribution map is generated for each image scene, with a unified colour scale and classification standard to ensure comparability of results across different years. The raster statistics and area calculation functions are then used to conduct

DOI: 10.54254/2755-2721/2026.33434

quantitative statistics on the spatial distribution of different heat island levels in each period, calculating the area and proportion of the strong green island zone, green island zone, normal zone, heat island zone and strong heat island zone, which are compiled into a statistical table of heat island level areas. On this basis, the four phases of heat island distribution maps and their area change data from 2010, 2015, 2020 and 2025 are compared to analyse the spatial expansion, contraction and shift of heat island areas of different levels, to identify the main change areas and evolution trend of the thermal environment pattern in Yinchuan City. Finally, by combining spatial distribution results and area statistics, a comprehensive analysis of the urban heat island effect in Yinchuan City from 2010 to 2025 is conducted. The temporal variation law and spatial distribution characteristics of heat island intensity are summarised, forming the final analysis results of urban heat island evolution in the study area.

3. Results

3.1. Spatial distribution characteristics

As shown in Fig. 3, the spatial distribution of heat islands in Yinchuan City deviates from the circular structure of traditional monocentric urban heat islands, exhibiting a distinct dumbbell-shaped spatial differentiation, with high temperatures at the northwest and southeast ends and a cool central area. The entire study area comprises natural heat sources in the northwest, industrial heat sources in the southeast, and a cold island matrix in the central area, embedded with urban patches.

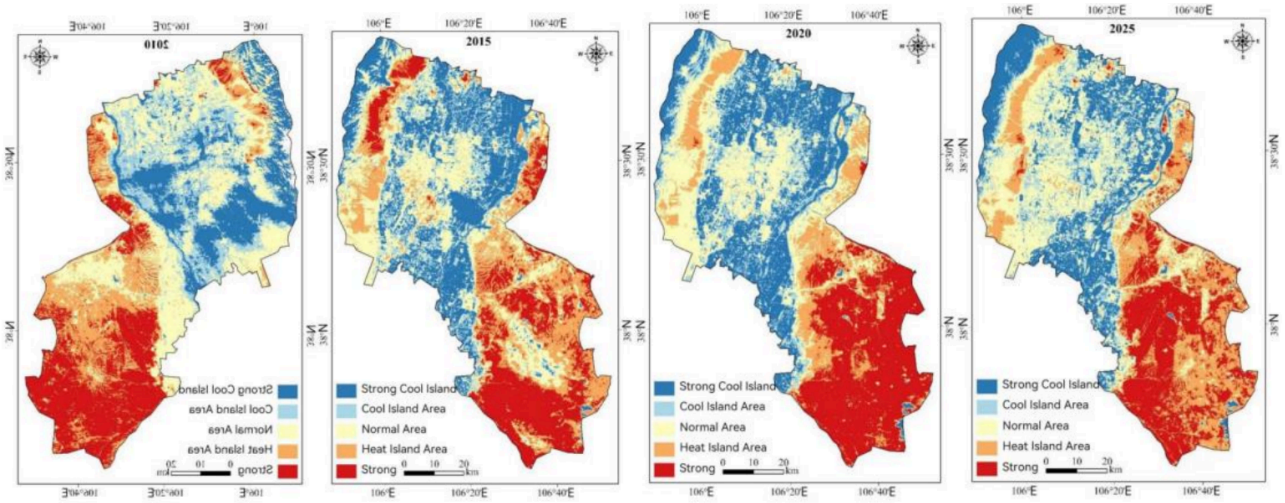

Figure 3. Heat island distribution of Yinchuan city from 2010 to 2025

3.2. Temporal variation results of heat islands

To quantitatively characterise the temporal evolution of the regional thermal environment, this study compiles statistics on the area changes for each heat island intensity level from 2010 to 2025 (Table 2).

In terms of temporal variation, the heat island intensity in Yinchuan City from 2010 to 2025 shows obvious phased fluctuation characteristics. As shown in Table 2, the area of the strong heat island zone has the most significant changes across different years. In 2010, the area of the strong heat island zone was 1427.30 km², accounting for 20.72% of the total area. It decreased slightly to 1308.08 km² in 2015, accounting for 18.80% of the total area. In 2020, the area of the strong heat

DOI: 10.54254/2755-2721/2026.33434

island zone increased significantly to 1714.86 km², accounting for 24.65%, the maximum value during the study period. In 2025, however, the area of the strong heat island zone decreased to 1311.27 km², accounting for 18.85% of the total area.

Table 2. Area statistics of heat island intensity levels across Yinchuan city from 2010 to 2025 (unit: km²)

Year	Strong Green Island Zone	Green Island Zone	Normal Zone	Heat Island Zone	Strong Heat Island Zone	Proportion of Strong Heat Island Zone
2010	1127.83	1050.17	2084.59	1197.02	1427.30	20.72%
2015	1483.99	918.35	1810.91	1435.84	1308.08	18.80%
2020	1563.90	947.00	1781.22	950.31	1714.86	24.65%
2025	1323.88	862.86	1976.50	1482.92	1311.27	18.85%

3.3. Spatial distribution characteristics of land use

The macro distribution pattern of land use and land cover significantly controls the spatial differentiation of LST in Yinchuan City. A comparison between the LST classification map and the region-wide land-use status shows that the macro outline of the thermal environment is highly consistent with the distribution boundaries of bare land, construction land, and agricultural, forest, and water areas. Differences in the thermal properties of the underlying surface across land-use types form the basic framework of the region-wide thermal environment.

To further reveal the spatial characteristics of the thermal environment, this study extracts the distribution of land-use types in Yinchuan City from 2010 to 2025 (Figure 4). The results show that different land-use types exhibit clear spatial differentiation: the northwest is dominated by bare land, the southeast by industrial construction land, and the central area by cropland, water bodies, and urban green spaces. A comparison of the heat island distribution results reveals that the strong heat island zones are concentrated in areas with dense bare land and construction land. In contrast, the green island zones correspond to water bodies and cropland, with high spatial consistency between the two.

Based on the spatial consistency analysis, zonal statistics are further conducted to assess heat island levels across different land-use types. The results show that the strong heat island zones are concentrated in construction land and bare land, with a higher area proportion than other land use types. In contrast, the green island zones are concentrated in water bodies and cropland. Overall, the distribution of land-use types across heat-island levels shows clear differences, indicating a strong correlation between land cover and land surface temperature.

DOI: 10.54254/2755-2721/2026.33434

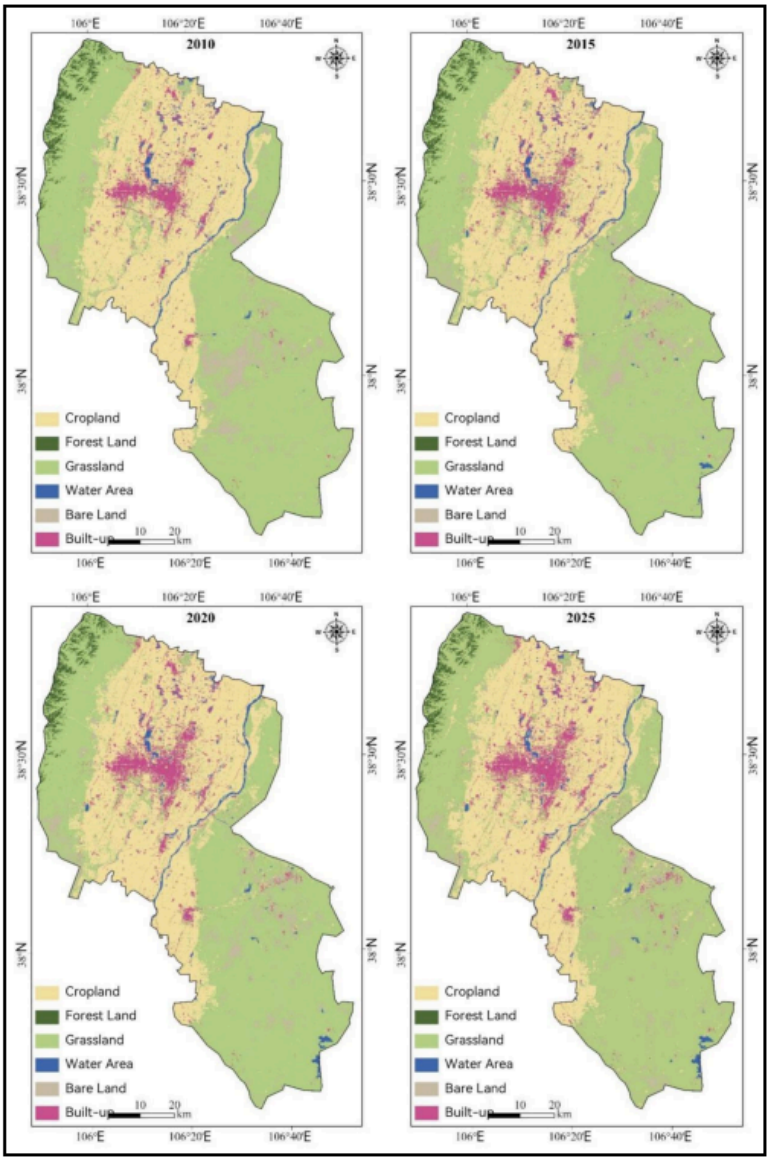

Figure 4: Land Use Types of Yinchuan City from 2010 to 2025

Figure 4. Land use types of Yinchuan city from 2010 to 2025

4. Analysis

4.1. Temporal variation mechanism of heat islands

Statistics reveal that the strong heat island zone saw the most dramatic changes between 2010 and 2025, with fluctuations in its area capturing the dynamic trade-off between the two major heat sources, the Helan Mountains in the northwest and Ningdong Base in the southeast, and the central cold island.

The temporal evolution of heat islands in Yinchuan exhibits distinct seasonal rhythms and is driven by the dual forces of urban expansion and industrial agglomeration. Seasonal background differences dominate the peak changes in heat island intensity, with the most typical contrast between July 2020 and October 2010. In 2020, the area of the region-wide strong heat island zone reached a peak of 1714.86 km², accounting for nearly 25% of the total area. This is because solar

DOI: 10.54254/2755-2721/2026.33434

radiation reaches its maximum in midsummer, with bare rocks in the Helan Mountains to the northwest, the desert in the Lingwu Platform to the southeast, and industrial facilities in Ningdong Base all experiencing extremely high temperatures simultaneously, creating a strong contiguous heat source across the entire study area. In autumn 2010, by contrast, industrial and urban heat sources remained. Still, natural mountains and deserts cooled rapidly with seasonal changes, resulting in a relatively small total area of the region-wide strong heat island zone. This presents a pattern in which natural heat sources weaken, and anthropogenic heat sources become dominant.

After accounting for seasonal factors, urban expansion and industrial agglomeration emerge as the main drivers of the evolution of thermal patches in the plain area. Between 2015 and 2025, westward and southward development of Jinfeng District led to the gradual expansion and coalescence of heat island patches in the central main urban area. This not only increased the total area of heat island zones, but also intensified encroachment on the surrounding cropland cold islands. Meanwhile, the continuous construction and expansion of the Ningdong Energy and Chemical Industry Base in the southeast, along with the growth of industrial impervious surfaces and exposed mining areas, kept high-temperature patches in this region in a stable, high-intensity distribution across all four image scenes [8]. The 2025 (June) data, however, show a fall in the area of the strong heat island zone. This is influenced not only by the fact that ground temperature has not yet accumulated in early summer, but also by the ecological restoration projects implemented in Yinchuan in recent years. In particular, desertification control in Lingwu Baijitan National Nature Reserve and green mine development in Ningdong Base have curbed the uncontrolled expansion of desert heat sources in the southeast to some extent, thereby consolidating the ecological security barrier for the region-wide thermal environment.

4.2. Analysis of the driving mechanism of land cover change on heat islands

4.2.1. Control effect of macro land use on the thermal environment

The radiative heating effect of the Helan Mountains alluvial fan is the direct cause of the formation of the high-temperature zone in the west. Across all four image scenes, the northwest maintains a stably distributed contiguous strong heat island zone, which corresponds to the alluvial fan and Gobi belt at the eastern foot of the Helan Mountains. The land surface in this area is mainly composed of exposed gravel and coarse sand, with no vegetation cover and scarce soil moisture, resulting in extremely low thermal inertia. Under intense daytime solar radiation, the dry gravel and sand surface heats up rapidly, forming the strongest natural heat source in the entire study area. These thermal properties, determined by geomorphology and lithology, are highly stable and do not shift fundamentally with urban development, forming the western high-temperature background of the region-wide thermal environment in Yinchuan.

The water regulation effect of the plain subsidence basin forms the geographical basis for the formation of the central cold island. As a Yellow River alluvial plain, the Yinchuan Plain has low, flat terrain, a shallow groundwater table, and a dense network of irrigation canals and lake wetlands, such as the Diannong River and Yuehai Lake. Water bodies and moist soil have a large specific heat capacity, and heat up slowly when receiving the same amount of solar radiation. This north-south cold source remains consistent in both autumn 2010 and midsummer 2020, confirming the strong buffering and stabilising effect of the plain's water and soil environment on the thermal environment.

DOI: 10.54254/2755-2721/2026.33434

4.2.2. Superposition and reshaping of local thermal environment by urban sprawl

On top of the macro natural thermal background, urbanisation has significantly superimposed on and reshaped the local thermal environment by altering the properties of the underlying surface. A comparison of LST imagery evolution between 2010 and 2025 clearly delineates the trajectory of how urban expansion drives changes in the thermal environment.

Coalescence of thermal patches caused by built-up area expansion is the main feature of changes in the thermal environment in the plain area. In the 2010 imagery, the heat island patches of Xingqing District (the old urban area) and Jinfeng District (the new urban area) have clear boundaries, with an obvious low-temperature buffer zone between them formed by undeveloped cropland and vacant land. By 2020 and 2025, however, with the implementation of the city's "east optimisation and west expansion" development strategy, the low-temperature buffer zone that originally separated the two districts was gradually filled by medium and high-temperature patches. This spatiotemporal change trajectory is highly consistent with the expansion direction of construction land in Yinchuan, indicating that the development of impervious surfaces, including buildings and roads, directly blocks the evaporative cooling pathways of the land surface. It connects originally scattered individual heat islands into contiguous zones, significantly increasing the region's heat accumulation intensity.

The heat-source intensification effect of industrial agglomerations is particularly pronounced in the southeast. In the Lingwu-Ningdong area, LST imagery reveals a long-term stable and extremely high-intensity core heat island. In addition to the natural desert background, this area is part of a high-intensity energy and chemical industry cluster. The high solar absorptivity of dark industrial underlying surfaces, such as coal stockyards and dark factory rooftops, combined with anthropogenic heat emissions from industrial production, creates a heat island effect driven by both natural and anthropogenic forces. The consistently high brightness of heat island patches in this area across the imagery is a direct reflection of the severe disturbance to the local thermal environment caused by industrialisation.

4.2.3. Regulation mechanism of seasonal climatic factors

In addition to long-term changes in land cover, the seasonal climatic background at the time of image acquisition is also an important factor driving short-term fluctuations in the thermal environment. The four image scenes selected for this study were acquired in early summer (June), midsummer (July), late summer (September), and mid-autumn (October), respectively, and seasonal changes have a significant regulatory effect on the thermal environment.

Seasonal differences in solar radiation intensity directly determine the strength of natural heat sources. In the midsummer imagery of July 2020, the region-wide area of the strong heat island zone reached its peak. This is because the high solar altitude angle and strong solar radiation in summer drive extremely intense heating of bare rocks in the western Helan Mountains and industrial zones in the east, thereby activating natural heat sources to the maximum extent. In the autumn imagery of October 2010, by contrast, as solar radiation weakens, the gravel surface, with its low specific heat capacity, cools rapidly. This leads to a significant contraction in the scope and intensity of the natural high-temperature zone in the west. At the same time, the outline of urban anthropogenic heat islands becomes more prominent instead. This phenomenon reveals that natural heat sources in arid zone cities are far more sensitive to seasonal changes than anthropogenic heat sources.

The influence of vegetation phenology is reflected in the strength of the central cold island. During the growing season (June to September) in 2015, 2020, and 2025, crops and urban greenery

DOI: 10.54254/2755-2721/2026.33434

in the plain area are in lush growth, with a strong transpiration cooling effect. This creates an extremely sharp contrast between the low-temperature zone in the central area and the high-temperature zones on both sides. In the autumn imagery of October, however, with crop harvesting and vegetation withering, the surface transpiration capacity decreases, and the temperature of exposed cropland rises, leading to a relative weakening of the central cold island effect.

5. Conclusion

The results show that the overall thermal environment of Yinchuan City exhibits a distinct dumbbell-shaped spatial structure, with high temperatures at the northwest and southeast ends and a relatively cool central area. This is significantly different from the circular pattern of traditional plain cities, which feature high temperatures in the urban centre and low temperatures in the periphery. The Helan Mountains alluvial fan in the northwest and the Lingwu-Ningdong Platform in the southeast consistently appear as high-temperature areas across multiple image scenes, forming the most stable and largest high-temperature background zone in the entire study area. The central Yinchuan Plain, by contrast, is relatively cool, presenting a thermal environment pattern where the urban area is embedded in an oasis matrix. In terms of temporal changes, the overall thermal environment of Yinchuan City between 2010 and 2025 shows a phased pattern of fluctuation, intensification, and decline, with the most pronounced changes in the area of the strong heat island zone. The region-wide area of the strong heat island zone reached its peak in the midsummer imagery of 2020, while the 2025 monitoring results show a decline in heat island intensity, indicating that the thermal environment of Yinchuan City exhibits obvious dynamic characteristics across different stages.

This study still has certain limitations. First, the analysis is based only on four phases of remote sensing imagery, with a relatively limited time series, making it difficult to fully reflect the long-term, continuous trend in heat island changes. Second, the imagery for different years was acquired in early summer, midsummer, late summer, and autumn, with differences in solar radiation intensity and background air temperature across seasons. Although the mean-standard deviation method reduces temperature background differences to some extent, seasonal factors may still affect the comparison of heat island intensity. In addition, Landsat imagery has a spatial resolution of 30 m, which may result in insufficient representation of local details in the city's complex underlying surface.

Future research can incorporate remote sensing data from additional years to build a more continuous time series, thereby further improving the temporal accuracy of analyses of urban heat island changes. At the same time, higher-resolution remote sensing imagery or multi-source remote sensing data can be combined to improve the level of refinement in thermal environment identification at the urban scale. In addition, future studies can combine meteorological observation data and urban microclimate research methods to conduct a more systematic analysis of changes in the urban thermal environment, thereby providing more reliable scientific reference for urban thermal environment monitoring and urban climate regulation.

References

[1] Oke, T. R. (1982). The energetic basis of the urban heat island. Quarterly Journal of the Royal Meteorological Society, 108(455), 1-24.

[2] Li, X., Zhou, Y., Yu, S., et al. (2019). Urban heat island impacts on building energy consumption: A review of approaches and findings. Energy, 174, 407-419.

DOI: 10.54254/2755-2721/2026.33434

[3] Wang, Z. Y., Kong, J. L., Li, Y., et al. (2021). Analysis of spatiotemporal characteristics of land surface evapotranspiration and its influencing factors in Yinchuan Plain based on MOD16. Hydrogeology & Engineering Geology, 48(3), 53-61.
[4] Gao, R. N., Zhu, X. W., Wang, F., et al. (2025). Evolution of urban heat island effect and evaluation of cooling effect of lake wetlands in Yinchuan City. Journal of Arid Meteorology, 43(1), 97.
[5] Zhang, H., Yang, Y. C., & Shi, K. B. (2017). Spatial pattern and driving mechanisms of the Islamization of the architectural landscape in Yinchuan City during the transitional period. Human Geography, 32(2), 37-45.
[6] Zhang, X. D., Zhao, Y. X., Wu, D., et al. (2020). Remote sensing-based analysis of urban expansion of built-up areas and its thermal environment changes in Yinchuan City. Arid Land Geography, 43(5), 1278-1288.
[7] Chen, S. L., & Wang, T. X. (2009). Comparative study on urban heat island delineation by equal interval method and mean-standard deviation method. Journal of Geo-information Science, 11(2), 145-150.
[8] Xu, Z. Y., Zhang, Y. T., Bu, C. D., et al. (2010). Analysis of land use change in Ningdong Energy and Heavy Chemical Industry Base based on RS and GIS. Soil and Water Conservation in China, (8), 66-67.